Phase-Sensitive Detection of Bragg Scattering at 1D Optical Lattices

S. Slama, C. von Cube, B. Deh, A. Ludewig, C. Zimmermann, and Ph. W. Courteille

Physikalisches Institut, Eberhard-Karls-Universität Tübingen, Auf der Morgenstelle 14, D-72076 Tübingen, Germany

(Received 22 October 2004; published 17 May 2005)

We report on the observation of Bragg scattering at 1D atomic lattices. Cold atoms are confined by optical dipole forces at the antinodes of a standing wave generated by the two counterpropagating modes of a laser-driven high-finesse ring cavity. By heterodyning the Bragg-scattered light with a reference beam, we obtain detailed information on phase shifts imparted by the Bragg scattering process. Being deep in the Lamb-Dicke regime, the scattered light is not broadened by the motion of individual atoms.

DOI: 10.1103/PhysRevLett.94.193901 PACS numbers: 42.65.Es, 32.80.Pj, 42.25.Fx

In the past, Bragg scattering has proven an extremely useful tool for observing and analyzing periodic structures such as crystals [1], molecules [2], or even artificial photonic band gap materials [3]. More recently, periodic lattice geometries have also been realized with ultracold atomic ensembles confined in optical standing waves [4]. However, optical Bragg scattering from such optical lattices has been investigated only for the special case of resonant lattices [5,6], where the optical trapping potential provides an efficient cooling mechanism for the trapped atomic cloud. In these experiments, the monitored power of the diffracted light yields information about the spatial distribution of the atoms. Cooling is important because it counteracts heating due to the applied probe light which destroys the atomic ordering. In far detuned optical lattices where cooling is absent, Bragg diffraction is thus very difficult and has not yet been studied. However, in combination with atomic degenerate quantum gases such purely conservative optical potentials provide intriguing perspectives for experimental modeling of solid state physics. The realization of a Mott insulator transition is one prominent example [7]. In this context, the successful application of Bragg diffraction methods would offer novel and powerful possibilities for sensitively probing the properties of such optical crystals. To minimize the destructive influence of resonant light absorption, the frequency of the probe laser beam could be detuned relative to an atomic resonance. Then, the information is mainly encoded in the phase shift imprinted by the sample onto the diffracted beam. In order to readout the phase, the diffracted light must be demodulated by superimposing a reference laser beam, and the beat signal can then be decomposed into its quadrature components. No such method has yet been demonstrated.

Such a scheme would be of particular value for investigating the feasibility of photonic crystals based on optical lattices. Usually, photonic crystals are periodic dielectric structures, which interact with light via Mie scattering. They can exhibit ranges of frequencies for which the propagation of light is classically forbidden [3]. Although impressive progress has been made in fabricating photonic crystals, they suffer from fundamental difficulties in providing the required fidelity over long ranges [8] due to fluctuations in the position and size of the building blocks. This disorder disturbs those properties of photonic crystals based on global interference: It reduces the Bragg reflectivity, extinguishes the transmitted light, and ultimately destroys the photonic band gap. On the other hand, optical lattices exhibit an intrinsically perfect periodicity. Local disorder introduced by thermal density fluctuations reduces the value of the Debye-Waller factor [9], but does not affect the quality of the long-range order. To observe photonic band gaps with optical lattices, one must reach the regime of multiple reflections of the incident light between adjacent layers. Unfortunately, this is not easy, because the efficiency of Bragg scattering is very weak except close to atomic resonances, where detrimental absorption due to disordered atoms limits the impact of coherent multiple reflections. Hence, it is important to identify clear signatures of multiple scattering in optical lattices and to develop sensitive tools for their detection. In the photonic band gap regime, the scattering of light is completely dominated by the dispersive part of the atomic polarizability [10], which is significantly strong also off resonance. We therefore expect that the scattering-induced phase shift contains sensitive signatures of multiple reflections and that its measurement will be essential for the detection of photonic band gaps in future experiments.

In this Letter, we report on the first direct measurement of the phase shift due to coherent scattering in a one-dimensional optical lattice. The elastic peak of the atomic response to incident laser light has been observed in several experiments. Westbrook *et al.* [11,12] used a heterodyne method to beat down the fluorescence of magneto-optically trapped atoms with a local oscillator to electronically accessible frequencies. However, in their experiment the heterodyne signal was integrated over long times, so that the phase coherence of the elastic scattering process is not directly observable. In contrast to previous experiments, we combine the techniques of Bragg scattering and heterodyning for constructing an interferometer: The frequency beat between the Bragg-reflected light and a reference laser having a different frequency is demodulated. From the two

quadrature components, we completely recover the complex scattering coefficient. We ramp the frequencies of both laser beams, the Bragg beam, and the reference beam simultaneously, so that the beat frequency is fixed. Because the elastically scattered light is always phase coherent, we can look for phase shifts due to the scattering process. At the same time, our experiment represents the first observation of Bragg scattering at 1D atomic density gratings.

The optical layout of our experiment is shown in Fig. 1. It consists of a high-finesse ring cavity, which has been discussed in Ref. [13], and a setup for Bragg scattering. The ring cavity has a finesse of 80 000 and a waist of $w_{\mathrm{dip}} = 130\ \mu$m. From a titanium-sapphire laser operating at $\lambda_{\mathrm{dip}} = 796$–$820$ nm, two light frequencies $\omega_{\pm}$ are generated by means of acousto-optic modulators (AOMs). The light beams pump the two counterpropagating modes of the ring cavity near resonance, thus forming a standing wave, which propagates at a velocity v given by $2k_{\mathrm{dip}}v = \omega_+ - \omega_-$. For most experiments reported here, we choose $\omega_+ = \omega_-$. The intracavity power is $P_{\mathrm{cav}} = 1$–10 W. Typically $N_{\mathrm{tot}} = 10^7$ ^{85}Rb atoms are loaded from a standard magneto-optical trap (MOT) into the standing wave close to the location of the waist, which is red detuned with respect to the rubidium D_1 line. The cloud is typically a few 100 μK cold.

The light of a blue laser diode (Toptica LD-0405-0005-2) operating at $\lambda_{\mathrm{brg}} = 420.2$ nm is split into a probe beam ω_i and a reference beam ω_r. The frequencies of the beams are controlled by means of AOMs. Some time after loading the atoms into the standing wave, the light beam ω_i is pulsed and shone under an angle of $\beta_i = 58°$ onto the atoms. The light reflected from the atoms, ω_s, is detected under the angle $\beta_s = -\beta_i$ with a photomultiplier (PMT) (Hamamatsu 1P28) terminated with a resistive load of $R = 100\ \mathrm{k}\Omega$. Some experiments were performed by carefully phase matching the Bragg beam with a reference beam ω_r (then the shutter S is open).

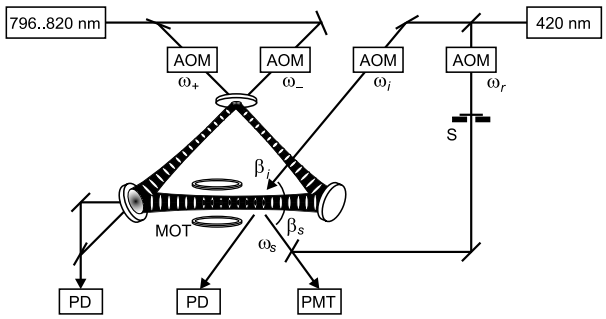

FIG. 1. The experimental setup consists of a ring cavity pumped at 796–820 nm and a diode laser at 420 nm for Bragg scattering. The shutter S controls the reference beam used to detect frequency beats between the Bragg and the reference beam. Photodiodes (PD) record the transmitted probe power and the beat note between the two cavity modes.

Our standing wave dipole trap represents a 1D optical lattice, whose periodicity is $\frac{1}{2}\lambda_{\mathrm{dip}} = \pi/k_{\mathrm{dip}}$. The Bragg condition requires $\lambda_{\mathrm{dip}}\cos\beta_i = \lambda_{\mathrm{brg}}$. To resonantly enhance the Bragg scattering, which otherwise would be negligibly small, we tune the laser to the transition $5S_{1/2}$, $F = 3 \rightarrow 6P_{3/2}$, $F' = 2, 3, 4$, with a natural linewidth of $\Gamma_{\mathrm{brg}}/2\pi = 1.3$ MHz [9]. During the Bragg pulse sequence, the repumping laser of the magneto-optical trap is shone onto the atoms to minimize optical pumping into the ground state $F = 2$ level.

The efficiency of Bragg scattering depends critically on the angle of incidence β_i: The acceptance angle is about $0.1°$. The scattered light beam has a nearly Gaussian elliptical shape. It is collimated in the scattering plane having about the same diameter as the input beam $w_z = 600\ \mu$m. This means that about $N_s \simeq 1500$ planes of the atomic lattice are illuminated, the lattice itself being longer. Therefore only a small fraction, $N \simeq N_{\mathrm{tot}}/5$, of the atoms confined in the dipole trap are illuminated by the Bragg beam. The radial size of the atomic cloud, $\sigma_r \approx 30\ \mu$m, determines the scattered beam divergence in the direction orthogonal to the scattering plane, $w_r = \sigma_r$. We calculate the solid angle $d\Omega_s$ in the far field, where both beams are divergent and the grating can be considered a point source as $\Omega_s \equiv 2\lambda_{\mathrm{brg}}^2/\pi w_r w_z \simeq 6 \times 10^{-6}$ sr.

The power P_s diffracted by Bragg scattering into a direction $d\Omega_s$ can be estimated from [9]

$$\frac{dP_s}{d\Omega_s} = I_i \frac{\pi^2}{\lambda_{\mathrm{brg}}^4} \left| \frac{\alpha}{\epsilon_0} \right|^2 \sin^2\xi \left| \sum_m e^{i\Delta\mathbf{k}\mathbf{R}_m} \right|^2 f_{\mathrm{DW}}^2, \qquad (1)$$

where

$$\alpha = \frac{6\pi\epsilon_0}{k_{\mathrm{brg}}^3} \frac{\Gamma_{\mathrm{brg}}}{2\Delta_{\mathrm{brg}} + i\Gamma_{\mathrm{brg}}} \qquad (2)$$

is the frequency-dependent complex polarizability. Δ_{brg} is the Bragg laser detuning. We actually use $I_i = 0.2\ \mathrm{mW/cm^2}$ incident intensity, which is about one-tenth of the saturation intensity I_{sat} and corresponds to the power $P_i = \frac{\pi}{2} w_z^2 I_i \approx 1\ \mu$W. The sum over individual atoms represents the structure factor, $\sum_m e^{i\Delta\mathbf{k}\mathbf{R}_m} = \sum_m e^{i2mk_{\mathrm{brg}}\lambda_{\mathrm{dip}}\cos\beta} = N_s$. The Bragg-scattered light power is proportional to the square of the atom number, as is verified in Fig. 2(a).

The Debye-Waller factor is given by $f_{\mathrm{DW}} = \overline{e^{i\Delta\mathbf{k}\mathbf{x}}} = e^{-(\Delta k_z)^2\sigma_z^2/2}$, since only the distribution of atoms along the lattice normal axis $\hat{z}$ contributes to the Debye-Waller factor, $\Delta k_{x,y} = 0$ and $\Delta k_z = 2k_{\mathrm{brg}}\cos\beta_i$. The rms size of the atomic cloud is $\sigma_z = k_{\mathrm{dip}}^{-1}\sqrt{k_B T/2U_0}$ in the harmonic approximation of the trapping potential. We noticed in earlier experiments [13,14] that the temperature of the cloud adopts a fixed ratio with the depth of the dipole trap, $T \approx 0.2U_0$. Therefore, the spatial distribution of the atoms (and thus the Debye-Waller factor) does not vary

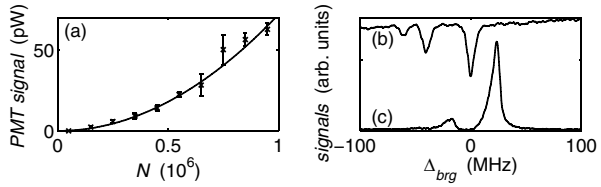

FIG. 2. (a) The quadratic dependence of the Bragg-scattered power P_s on the atom number N agrees well with Eq. (1). (b) Absorption spectrum of magneto-optically trapped atoms showing the hyperfine levels $F' = 2, 3, 4$. (c) Bragg reflection spectrum obtained by ramping the blue laser frequency. Here the shutter S in Fig. 1 blocked the reference beam. Only the two strongest hyperfine peaks are visible.

much with temperature, so that we estimate $f_{\mathrm{DW}} = 0.8$. Finally, the angle between the polarization of the incident light and the diffracted wave vector is chosen to be $\xi = 90°$. With the above estimations, we calculate for the scattered power on resonance from Eq. (1) $P_s \simeq 150$ nW.

Figure 2(c) shows a spectrum of the Bragg resonance obtained by ramping the laser frequency at 420 nm (with the shutter S closed). Three hyperfine components are expected in the spectrum, i.e., $F' = 2, 3, 4$. However, the $F' = 2$ component is too weak to be seen. Figure 2(b) shows a MOT absorption spectrum for reference. The frequency displacement between the spectra is due to the light shift of the atoms in the dipole trap.

The *measured* peak power of the Bragg-reflected light is on the order of $P_{s,m} = 100$ pW. During a scan of typically 6 ms duration, the laser spends roughly $\Delta t = 1$ ms close to the strongest resonance line, which is sufficient to scatter $\Delta t P_{s,m}/\hbar\omega_s \simeq 200\,000$ photons. Defining the reflectivity as the ratio of the scattered power and the fraction of power incident on the atoms (i.e., reduced in order to account for the partial overlap between the incident beam and the atomic cloud), $R = P_{s,m}/(\frac{1}{2}\pi w_r w_z I_i)$, we obtain for the amplitude reflection coefficient $|r| = \sqrt{R} \simeq 3\%$.

The discrepancy between the calculated and the measured Bragg-reflected power, which has also been observed in [6], is due to a combination of two effects: First, the dipole-trapped atoms are subject to a position-dependent Stark shift, which inhomogeneously broadens the Bragg spectrum. This effect, which depends on the potential depth U_0 and the temperature T, leads to asymmetric resonance peaks, as seen in Fig. 2(c). From calculations, we estimate a line broadening of about $10\Gamma_{\mathrm{brg}}$, resulting in a strong reduction of the Bragg-reflected light peak intensity. Second, incoherent processes occur at a rate of $(I_i/I_{\mathrm{sat}})(1 + 4\Delta_{\mathrm{brg}}^2/\Gamma_{\mathrm{brg}}^2)^{-1} \lesssim 0.5$ times the elastic scattering rate. These processes cause heating and optical hyperfine pumping. In fact, we observe noticeable depletion of the lattice when scanning the blue laser over the resonance. Experimentally, we reduce the light power and increase the scanning speed to avoid distortion of the line profile due to heating during a scan.

The spectroscopy detailed above yields only the absolute value of the reflection coefficient $|r|$. To also measure its phase, we phase match the Bragg beam with a reference laser beam and observe the frequency beat on the PMT signal. By passing the beam shone onto the atomic cloud, ω_i, and the reference beam, ω_r, through acousto-optic modulators (see Fig. 1), we can arbitrarily chose the beat frequency. We expect to see the frequency component $\Delta\omega_i \equiv \omega_i - \omega_r$ in the beat signal. A typical spectrum is shown in Fig. 3(a).

Laser frequency fluctuations limit the resolution of the spectrum. On a long time scale the laser emission bandwidth is estimated to less than 5 MHz. However, the time scale on which the spectrum is recorded (a few milliseconds) is so short that the acoustic noise does not completely inhibit phase-sensitive detection.

When light is scattered at an unbound atomic cloud, the elastic Rayleigh peak is Doppler broadened by the recoil imparted to the atoms, whose velocities have a Maxwell-Boltzmann distribution. However, in axial direction the atoms are localized to less than $\sigma_z \ll \lambda_{\mathrm{dip}}/2 < \lambda_{\mathrm{brg}}$, so that the resonance fluorescence spectrum is Dicke narrowed. The rate of inelastic scattering events in which the vibrational quantum number changes is reduced by the Lamb-Dicke factor $(2n_z + 1)\epsilon/\Omega_z \approx 0.01$, where n_z is the vibrational quantum number for axial atomic oscillation, Ω_z the oscillation frequency, and ϵ is the recoil

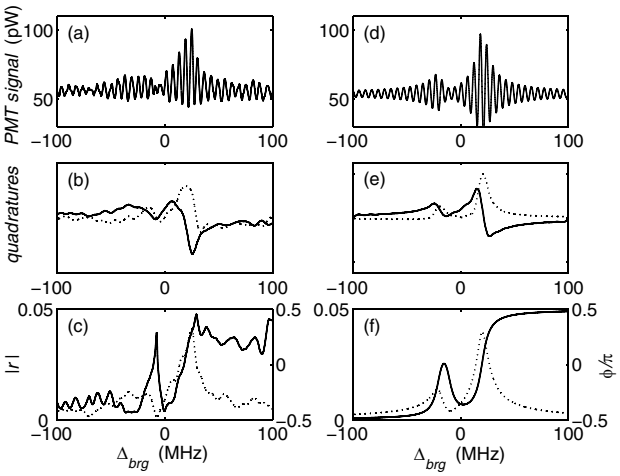

FIG. 3. (a) Beat signal recorded while tuning the blue laser across resonance. The frequencies were chosen such that $\Delta_i/(2\pi) = 5.4$ kHz. (b) Quadrature components of the beat signal and (c) amplitude profile calculated from the quadrature components and phase profile as obtained by counting the number of oscillations in (a) per time interval. (d) Simulated beat signal spectrum between Bragg-scattered light and a reference beam using a calculated amplitude and phase profile. (e) Quadrature components of the Bragg beat demodulated with the reference beat. (f) Amplitude (dashed line) and phase profile (solid line) as derived from the quadrature components. The profiles coincide with the profiles used to calculate the curves in (d).

frequency. Elastic scattering events involving no change in vibrational level are favored. The spectrum is thus Doppler-free, and we do not expect recoil shifts.

The complex scattering amplitude $r = |r|e^{i\phi}$ represents the global response of the atomic cloud to an incident laser $E_i = E_{i0}e^{i\omega_i t}$. Thus the Bragg-scattered light is given by $E_s = rE_i = |r|E_{i0}e^{i\omega_i t + i\phi}$. While the amplitude $|r|$ is obtained via simple absorption spectroscopy, acquiring phase information $\phi(t)$ needs heterodyning. Therefore we beat the Bragg-scattered light with a reference beam $E_r = E_{r0}e^{i\omega_r t}$ while scanning over the resonance $I = |E_r + E_s|^2$. We obtain $I \approx E_{r0}^2 + |r|^2 E_{i0}^2 + 2|r|E_{r0}E_{i0}\cos(\Delta\omega_i t + \phi)$.

In order to calculate amplitude and phase from a beat signal spectrum shown in Fig. 3(a), we extract the quadrature and the in-phase component by numerically demodulating the beat signal with $\cos\Delta\omega_i t$ and $\sin\Delta\omega_i t$. Low-pass filtering the dc components yields $\bar{U}_s = -|r|E_{r0}E_{i0}\sin\phi$ and $\bar{U}_c = |r|E_{r0}E_{i0}\cos\phi$. Figure 3(b) shows the quadrature components. Phase and amplitude follow from $rE_{r0}E_{i0}(t) = (\bar{U}_c{}^2 + \bar{U}_s{}^2)^{1/2}$ and $\tan\phi(t) = -\bar{U}_s/\bar{U}_c$. The result is shown in Fig. 3(c). We notice an absorptive profile for the reflection amplitude, which coincides with the profile recorded without heterodyning (shutter S is closed) [see Fig. 2(c)]. The dispersively shaped phase profile in Fig. 2(c) exhibits a maximum phase shift on the order of π and a distortion due to the hyperfine splitting of the upper level.

To describe the observation, we calculate the complex reflection coefficient $r \propto \alpha$ for our lattice and use it to simulate the beat signal shown in Fig. 3(d). This signal, if submitted to the same data processing as for the experimental data, yields the curves in Figs. 3(e) and 3(f). In particular, the amplitude and the phase profile of Fig. 3(f) exactly recover the calculated complex reflection coefficient. To compare with the experiment, we adjust the power values in the modes $E_r \approx E_i \simeq 54$ pW. We notice a good agreement, despite the noise appearing in the measured data. This noise is due to frequency fluctuations of the blue laser beam and to variations in the position of the ring cavity standing wave.

The phase delay is intrinsically connected with the Rayleigh scattering process, which predicts a phase shift described by $\tan\phi = \mathrm{Im}\alpha/\mathrm{Re}\alpha = -\Gamma_{\mathrm{brg}}/2\Delta_{\mathrm{brg}}$, i.e., the phase evolves from $\phi = 0$ to $-\pi$ across the resonance as shown in Fig. 3(f). Additional phase shifts may, in principle, result from the finite propagation time of the incident beam slowed down by refractive index variations in the optically dense cloud, and from multiple scattering between the atomic layers. In our case, the finite radial size of the scattering layers limits the effective number of layers participating in multiple scattering to $N_{\mathrm{eff}} = 2w_r/\lambda_{\mathrm{dip}}\tan\beta_i \simeq 160$. We estimate our mean density as $n = 5 \times 10^{11}$ cm^{-3}. In this thin grating regime, the above effects are not expected to contribute to the observed signals. We verified this assumption by calculating the complex reflection coefficient using a transfer matrix formalism [10], and we found identical results.

In conclusion, periodic ordering in atomic clouds can have dramatic influence on the propagation and scattering of light. For thin atomic lattices, the Rayleigh scattered light destructively interferes in all but one direction. The resonant enhancement of Rayleigh scattering in this direction provided us with enough intensity to realize a ''Bragg interferometer'' in an atomic gas. This method may prove sufficiently accurate for probing interesting features of Bragg scattering in the limit where multiple reflections between adjacent layers are frequent, such as the occurrence of photonic band gaps for certain ranges of light detuning or incident angles [10].

Interferometric techniques are ideally suited for measuring propagation velocities. By supplying different pump frequencies for the counterpropagating modes, $\omega_+ \neq \omega_-$, we can rotate the standing wave in the ring cavity. We measure the resulting Doppler shift of the light Bragg scattered at the atomic grating with an accuracy better than 1%. An interesting application of this method could be the study of self-organized systems. Under certain circumstances, atomic ensembles driven by dissipative forces spontaneously arrange themselves into propagating periodic lattices [15], whose bunching and propagation velocity could conveniently be detected.

We acknowledge financial support from the Landesstiftung Baden-Württemberg.

[1] E. O. Wollan, Rev. Mod. Phys. **4**, 205 (1932).
[2] J. Doucet and J. P. Benoit, Nature (London) **325**, 643 (1987).
[3] S. John and M. J. Stephen, Phys. Rev. B **28**, 6358 (1983).
[4] P. S. Jessen and I. H. Deutsch, Adv. At. Mol. Opt. Phys. **37**, 95 (1996).
[5] G. Birkl *et al.*, Phys. Rev. Lett. **75**, 2823 (1995).
[6] M. Weidemüller *et al.*, Phys. Rev. Lett. **75**, 4583 (1995).
[7] M. Greiner *et al.*, Nature (London) **415**, 39 (2002).
[8] A. F. Koenderink and W. L. Vos, Phys. Rev. Lett. **91**, 213902 (2003).
[9] M. Weidemüller, A. Görlitz, Th. W. Hänsch, and A. Hemmerich, Phys. Rev. A **58**, 4647 (1998).
[10] I. H. Deutsch, R. J. C. Spreeuw, S. L. Rolston, and W. D. Phillips, Phys. Rev. A **52**, 1394 (1995).
[11] C. I. Westbrook *et al.*, Phys. Rev. Lett. **65**, 33 (1990).
[12] P. Jessen *et al.*, Phys. Rev. Lett. **69**, 49 (1992).
[13] D. Kruse *et al.*, Phys. Rev. A **67**, 051802(R) (2003).
[14] B. Nagorny *et al.*, Phys. Rev. A **67**, 031401(R) (2003).
[15] D. Kruse, C. von Cube, C. Zimmermann, and Ph. W. Courteille, Phys. Rev. Lett. **91**, 183601 (2003).